Optimization of Gasoline Compression Ignition Combustion with Ozone Addition and Two-stage Direct-Injection at Middle Loads

Yoshimitsu Kobashi[1]*, Tu Dan Dan Da[1], Ryuya Inagaki[1], G. Shibata[1], H. Ogawa[1]

[1] Division of Energy and Environmental Systems, Graduate School of Engineering, Hokkaido University, Japan

Abstract

Ozone (O_3) was introduced into the intake air to control the ignition in a gasoline compression ignition (GCI) engine. An early fuel injection at -68ºCA ATDC was adopted to mix the fuel with the reactive O-radicals decomposed from the O_3, before the reduction of the O-radicals due to their recombination would take place. The second injection was implemented near top dead center to optimize the profile of the heat release rate. The engine experiments were performed around the indicated mean effective pressure (IMEP) of 0.67 MPa with a primary reference fuel, octane number 90 (PRF90), maintaining the 15% intake oxygen concentration with the EGR. The quantity of the first injection, the second injection timing as well as the ozone concentration were changed as experimental parameters. The results showed that the GCI operation with the ozone addition makes it possible to reduce the maximum pressure rise rate while attaining high thermal efficiency,

* Corresponding author at: Kita 13, Nishi 8, Kita-ku, Sapporo, Hokkaido, Japan

E-mail address: kobashi@eng.hokudai.ac.jp (Yoshimitsu Kobashi)

compared to that without the ozone. Appropriate combinations of the ozone concentration and the first injection quantity achieve low smoke and NO_x emissions. Further, the ozone-assisted GCI operation was compared with conventional diesel operation. The results showed that the indicated thermal efficiency of the ozone-assisted GCI combustion is slightly lower than that of the conventional diesel combustion, but that GCI assisted with ozone is highly advantageous to the smoke and NO_x emissions.

Keywords: Gasoline Compression Ignition Engine, Ozone, Two-stage Injection, Thermal Efficiency, Exhaust Emissions

Nomenclature:

CDC	Conventional diesel combustion
GCI	Gasoline compression ignition
HCCI	Homogeneous charge compression ignition
HTOR	High temperature oxidation reaction
	"First HTOR" stands for the HTOR of the first injection fuel
	"Second HTOR" stands for the HTOR of the second injection fuel
LTOR	Low temperature oxidation reaction
RCCI	Reactivity controlled compression ignition
ROHR	Rate of heat release
TDC	Top dead center
$(dp/d\theta)_{max}$	Maximum pressure rise rate [MPa/ºCA]
p_{inj}	Injection pressure [MPa]
$Q_{inj.1st}$	Mass ratio of first injection [%]

X_{O3}	Concentration of ozone (O_3) in the intake air [ppm]

Greek symbols:

ϕ_{exh}	Exhaust loss [%]
ϕ_{other}	Other losses [%] equivalent to cooling loss
η_i	Indicated thermal efficiency [%]
η_{comb}	Combustion efficiency [%]
$\theta_{inj.1st}$	First injection timing [ºCA ATDC]
$\theta_{inj.2nd}$	Second injection timing [ºCA ATDC]
$\tau_{ign.2nd}$	Ignition delay of second injection [ºCA]

1. Introduction

1.1 Background

Compression ignition engines offer superior fuel economy. However, in diesel engines, achieving reductions in exhaust emissions remains a problem, as a turbulent diffusion flame surrounds the fuel spray, generating nitrogen oxide (NO_x), and as there is soot formation in the fuel rich central reaction zone [1-2]. The low reactivity of gasoline is advantageous to extend a no flame region between the tip of the fuel injector and the uppermost stream in a turbulent diffusion flame. The length of this zone (from the injector to the flame, elsewhere termed the lift-off length or as here the set-off length) plays a significant role in the soot formation as air is entrained and mixed with the fuel upstream of the set-off length [3-7]. Gasoline has the further benefit to form leaner mixtures due to

its high volatility. Considering these features, compression ignition engines using gasoline have attracted increasing attention as alternatives to diesel engines due to the potential for low emissions and high thermal efficiencies [8-11].

Unlike homogeneous charge compression ignition (HCCI) in which a homogeneous mixture is ignited, gasoline compression ignition (GCI) is believed to be advantageous to enable better ignition control as the injection is implemented near top dead center (TDC), and as the ignition timing is closely coupled to the injection timing. In practice, however, achieving ignition control over a wide range of engine loads and rotation speeds is challenging as the low reactivity of gasoline increases the dependence of the ignition process of GCI on the time scale of chemical reactions. One approach to control the ignition process of GCI is to employ a multiple-injection strategy, where the fuel injected at an early timing produces reactive radicals, and increases the in-cylinder temperature before TDC, decreasing the ignition delays of the fuel injected subsequently [10-13]. A more effective approach is to introduce reactive chemical species into the intake. Ozone (O_3) may be a potential candidate for this, and it has been investigated for ignition control in HCCI engines [14-18]. Chemical kinetic studies have shown that ozone decomposes at around 600 K, and that O-radicals are generated via the decomposition as follows [19-20]:

87 $O_3 + M = O_2 + O + M$ (R1)

88 The O-radicals reduce the onset temperature of the low temperature heat release, and
89 promote the ignition. The generated O-radicals, however, immediately recombine, to
90 form O_2 as:

91 $O + O + M = O_2 + M$ (R2)

92 This diminishes the impact of the ozone addition on the ignition process of the fuel. The
93 experimental study by Ekoto and Foucher have elucidated the reaction mechanism in a
94 single cylinder engine with an optical diagnostic approach [21].

95 **1.2 Methodology and Purpose of the Present Study**

96 Employing a two-stage injection strategy with an early first injection makes it possible
97 to utilize the reactive O-radicals [22], as shown in Fig.1. (a) The ozone-enriched air is
98 introduced at the intake stroke. (b) The first fuel injection is implemented before the ozone
99 decomposition takes place. (c) The fuel reacts with the O-radicals decomposed from the
100 ozone, and produces reactive radicals. (d) Near TDC, the fuel is injected into the
101 combustion chamber when the reactive radicals are present. This would cause a reactivity
102 stratification in the chamber as proposed in the reactivity controlled compression ignition
103 (RCCI) strategy [23]. The presence of the reactive radicals is advantageous in terms of

104 the combustion efficiency as examined in previous work [24]. A further potential
105 advantage with this strategy is the ability to control ignition delays and set-off length of
106 the second injection, enabling soot formation control.

107 A similar two-stage injection strategy with ozone addition has been proposed by
108 Pinazzi and Foucher aiming to improve low load operation of GCI engines [25], in the
109 present study, however, the GCI operation is extended to higher engine loads.

110 By examining the effects of the ozone concentration and the mass ratio between the
111 first and second injections, the advantage over the conventional GCI combustion is
112 elucidated. Smoke emissions are correlated with the ignition delays of the second
113 injection to evaluate the possibility of set-off length control. Finally, the performance of
114 GCI with the ozone addition is compared with that of diesel combustion employing a high
115 pressure injection strategy.

116 2. Experimental Setup and Procedures

117 An illustration of the experimental setup detailed in the previous paper [22] is shown
118 in Fig.2. The test engine was a single cylinder diesel engine equipped with a low pressure
119 EGR pathway and a roots type blower (OGURA CLUTCH, TX04) for supercharging. A
120 common-rail fuel injection system was used, employing a commercially available injector

121 (DENSO, G4S) and an 8-hole nozzle with nominal hole diameters of 0.125 mm and an
122 umbrella angle of 155º. The specifications of the test engine are detailed in Table 1. The
123 bore and stroke are 98 mm and 110 mm, and the displacement volume is 830 cm^3, the
124 compression ratio is 17.6.

125 A piezoelectric pressure sensor (KISTLER, 6125B) was installed in the cylinder head,
126 and the electrical charge produced by the piezoelectric sensor was converted into a
127 voltage signal with a charge amplifier (KISTLER, 5011B). The voltage signal
128 proportional to the cylinder pressure was recorded with a transient memory board at a
129 resolution of 0.2ºCA for 150 cycles.

130 Ozone (O_3) was produced with an ozonizer (EcoDesign, ED-OG-S4AD) while
131 introducing pure oxygen (O_2) from a gas cylinder, and it was delivered into the intake
132 pipe (diameter: 52.7 mm), located 450 mm upstream of the intake port. The volume from
133 the gas inlet to the intake port was larger than the displacement volume, and it was
134 assumed that the ozone-containing oxygen were homogeneously dispersed in the
135 combustion chamber.

136 The ozone concentration was measured with a UV ozone monitor (EBARA, EL-600)
137 before the ozone-containing oxygen was introduced into the intake pipe. The volume-
138 based ozone concentration X_{O3} in the intake air was determined with the measured O_3

139 concentration and the flow rates of the oxygen, and the intake air which was determined
140 using a differential pressure type flowmeter.

141 The concentrations of the total hydrocarbon (THC), carbon monoxide (CO), carbon
142 dioxide (CO_2), nitrogen oxide (NO_x), and oxygen (O_2) were measured at the intake and
143 exhaust pipes with an exhaust gas analyzer (Best Sokki, BEX-5100D). The smoke
144 emissions were measured with a Bosch-type smoke meter (ZEXEL, DSM-20AN).

145 The definitions of the ignition timing and ignition delay of the second injection $\tau_{ign.2nd}$
146 are shown in Fig.3. In most cases in the present study, a two-stage combustion occurred.
147 The first combustion, termed the first HTOR here, is due to the high temperature oxidation
148 reaction (HTOR) of the first fuel injection, and the second, termed the second HTOR, is
149 due to the HTOR of the second fuel injection. The profiles of the rates of heat release
150 (ROHR) due to the first and second HTOR were often overlapping. To determine the
151 ignition timing of the second injection, the ROHR due to the first HTOR (B) was
152 subtracted from the as-recorded ROHR (A), and the ROHR due to the second HTOR (C)
153 was inferred. Assuming a Gaussian distribution in the ROHR profile of the first HTOR,
154 the ROHR profile was inverted at the peak as suggested by the red and green parts of the
155 curves. The ignition timing of the second injection was determined as the derivative of
156 the ROHR of the second injection exceeded 15 J/^{o}CA^2, and the ignition delay of the

second injection $\tau_{ign.2nd}$ was defined to be from the start of the second injection $\theta_{inj.2nd}$ to the ignition of the fuel introduced in the second injection.

3. Results and Discussion

3.1 Experimental Conditions

The experimental conditions are detailed in Table 2. The fuel used in the present study is a mixture of primary reference fuels: i-octane (i-C_8H_{18}) and n-heptane (n-C_7H_{16}), and the mixed-in fraction of i-octane in the liquid phase is 90 vol.%, which is termed PRF90, as detailed chemical kinetic models of primary reference fuels have been developed, and it is possible to investigate the effects of chemical reactions due to the ozone addition in the future work.

The engine speed was maintained at 1200 rpm. In the previous studies, ozone was applied to improve low load operation of GCI [22, 25]. To examine the benefit of the ozone addition at higher loads, the total injection quantity was set to 29 mg/cycle, and the resultant indicated mean effective pressure (IMEP) was around 0.67 MPa, at the conditions here. As the ozone chemistry mainly affects the low temperature oxidation reaction (LTOR), its interaction depends on the equivalence ratio. It may be interesting to investigate the effects of injection pressure, affecting the equivalence ratio, on the ozone

174 chemistry interaction, but the present study set the injection pressure p_{inj} to 80 MPa,
175 considering the current situation in GCI engines.

176 The ratio of the first injection quantity $Q_{inj.1st}$, defined as the ratio of fuel in the first
177 injection with respect to the total fuel injected, as well as the ozone concentration X_{O3} was
178 changed as the experimental variables, to examine the effects on the ignition timings of
179 the second injection. In the previous study, retarding the first injection timing $\theta_{inj.1st}$
180 decreases the quantity of heat release by the first injection, even remarkable so later than
181 -60ºCA ATDC, showing that the O-radicals decomposed from ozone missed an
182 opportunity to react with the first injection [22]. Considering this and the fact that too
183 early injection may cause wall-wetting, the first injection timing $\theta_{inj.1st}$ was set at -68ºCA
184 ATDC. The second injection timing $\theta_{inj.2nd}$ was advanced from 6ºCA ATDC until the local
185 maximum of the indicated thermal efficiency was identified. The operation was limited
186 by the thresholds of the maximum pressure rise rate $(dp/d\theta)_{max}$ less than 1.0 MPa/ºCA, or
187 when operation became unstable.

188 The intake oxygen concentration, determined to attain NO_x less than 100 ppm in a
189 typical condition, was maintained at 15% with the EGR. By reference to situations in
190 automotive engines at middle loads, the intake air pressure was set at 120 kPa (abs.),
191 maintaining the exhaust gas at the same pressure by throttling the valve at the exhaust

192 pipe. Assuming the increase in the temperature due to the turbocharging, the intake air
193 temperature was set at 60ºC.

194 **3.2 Effects of the Ozone Concentration**

195 Figure 4 shows the profiles of the in-cylinder pressure and rate of heat release
196 (ROHR), changed with the ozone concentration X_{O3}, where the ratio of the first injection
197 quantity $Q_{inj.1st}$ and the second injection timing $\theta_{inj.2nd}$ was set at 35% and at TDC. The
198 small heat release due to the low temperature oxidation reaction (LTOR) of the first
199 injection fuel was identified before -20ºCA ATDC. The heat release appearing near TDC
200 was due to the high temperature oxidation reaction (HTOR) of the first injection fuel (first
201 HTOR), and subsequently the HTOR of the second injection fuel (second HTOR)
202 occurred. With the increase in the ozone concentration X_{O3}, the ROHR in the first HTOR
203 increased, causing an advance in the second HTOR. The ROHR in the second HTOR
204 increased from X_{O3} = 30 ppm to X_{O3} = 60 ppm due to the advanced combustion phasing.
205 A further increase of the ozone concentration decreased the ROHR in the second HTOR
206 due to the decreased ignition delay of the second injection, coupled with the effects of the
207 decrease in fuel available for the second HTOR.

208 Figure 5 shows the indicated thermal efficiency η_i, combustion efficiency η_{comb},

209 exhaust loss ϕ_{exh}, and other losses ϕ_{other} at the fixed ratio of the first injection quantity
210 $Q_{inj.1st}$ of 35%. Here, the other losses ϕ_{other} are equivalent to the cooling loss. The
211 combustion efficiency was improved with the increase in the ozone concentration X_{O3}. As
212 the source of the unburned emissions may be the lean mixture formed by the first injection,
213 this result suggests that the ozone addition improves the reactivity of the lean mixture.
214 The retarded second injection timing $\theta_{inj.2nd}$ deteriorated the combustion efficiency, and
215 increased the exhaust loss due to the retarded combustion phasing. With the increase in
216 the ozone concentration X_{O3}, the combustion phasing advanced as seen in Fig.4, followed
217 by a decrease in the exhaust loss, and an increase in the other losses. As the balance
218 between these effects, the maximum indicated thermal efficiency was achieved with X_{O3}
219 = 60 ppm and 120 ppm.

220 **3.3 Effects of the Ratio of the First Injection Quantity**

221 Figure 6 shows the profiles of the rate of heat release (ROHR), changed with the
222 second injection timing $\theta_{inj.2nd}$, for different ratios of the first injection quantity $Q_{inj.1st}$.
223 Here, the ozone concentration X_{O3} attaining high thermal efficiency was selected with
224 respect to each $Q_{inj.1st}$. The experiments were implemented under the following
225 conditions; 120, 180, 240, 300, and 360 ppm for the $Q_{inj.1st}$ of 20%; 30, 60, 120, and 180

226 ppm for the $Q_{inj.1st}$ of 35%; 10, 30, 60, and 120 ppm for the $Q_{inj.1st}$ of 50%; 0, 10, and 30
227 ppm for the $Q_{inj.1st}$ of 60%, while changing the second injection timing. These conditions
228 were chosen to find local maximum values of the indicated thermal efficiency with
229 respect to the change in the ozone concentration. In the case of the $Q_{inj.1st}$ of 60%, there
230 was no significant differences in the maximum indicted thermal efficiency between the
231 ozone concentrations X_{O3}, so that X_{O3} = 0 ppm was selected here for a comparison purpose.
232 The X_{O3} decreased with the increase of the $Q_{inj.1st}$ from 300 ppm to 0 ppm, and stable GCI
233 operation without ozone (X_{O3} = 0 ppm) were achieved with the $Q_{inj.1st}$ of 60%. The second
234 injection timing $\theta_{inj.2nd}$ achieving the maximum indicated thermal efficiency is that
235 underlined in the figure.

236 The late combustion phasing was identified with the ratio of the first injection quantity
237 $Q_{inj.1st}$ of 20%. This is because the ROHR in the first HTOR, which occurred near TDC,
238 was very small. The ROHR in the first HTOR increased with the increase in the first
239 injection $Q_{inj.1st}$ from 20% to 50%, advancing the second HTOR. With the $Q_{inj.1st}$ at 60%,
240 in the absence of ozone, the first HTOR occurred after TDC, and the first and second
241 injection fuels burned simultaneously with the second injections before the $\theta_{inj.2nd}$ of TDC,
242 causing the sudden elevation in the ROHR.

243 Figure 7 shows the indicated thermal efficiency η_i, combustion efficiency η_{comb},

exhaust loss ϕ_{exh}, and other losses ϕ_{other} for different ratios of the first injection quantity $Q_{inj.1st}$. The data shown in this figure were acquired under experimental conditions identical to those in Fig.6, except for the data acquired at the $Q_{inj.1st}$ of 60% and $\theta_{inj.2nd}$ of -4ºCA ATDC, which is added to show the trend including the knocking condition.

The advance of the second injection improved the indicated thermal efficiency as the combustion phasing was advanced, and the exhaust loss decreased. The $Q_{inj.1st}$ of 60% achieved the lowest exhaust loss as the combustion phasing was early (see Fig.6), and combustion periods were shorter than the others. The combustion efficiency with the $Q_{inj.1st}$ of 60% was lower than that with the $Q_{inj.1st}$ of 35% and 50% due to the absence of ozone. With the $Q_{inj.1st}$ of 60%, a further increase of the ozone concentration can increase the combustion efficiency and thermal efficiency at the second injection timings later than TDC, but the combustion phasing would be too far advanced against the early second injection timings, causing deterioration of the thermal efficiency. A further increase of the ozone concentration along with decreases of the intake oxygen concentration and intake air pressure may be a possible way to increase the combustion efficiency and to optimize the combustion phasing for the early second injections. With the $Q_{inj.1st}$ of 20%, the late combustion phasing deteriorated the combustion efficiency and exhaust loss, and caused the unstable operation, while advancing the second injection improved the combustion

262 efficiency due to the advanced combustion phasing, coupled with the combustion
263 enhancement effects induced by the higher concentration of ozone.

264 The $Q_{inj.1st}$ of 60% yielded the higher other losses value. The larger quantity in the
265 first injection may increase the cooling loss as the combustion temperature of the mixture
266 which is widely spread throughout the combustion chamber increases. In addition, the
267 rapid combustion of the $Q_{inj.1st}$ of 60% may increase the cooling loss due to increased wall
268 heat transfer. The other losses with the $Q_{inj.1st}$ of 50% were slightly higher than that with
269 the $Q_{inj.1st}$ of 35%, but the differences were rather small, and increased from $Q_{inj.1st}$ of 35%
270 to 20%. This may be because the momentum of the spray flame increased with the
271 increase of the second injection quantity, and more of the spray flame impinged on the
272 piston wall, enhancing the heat transfer to the wall.

273 Overall, this suggests that with the $Q_{inj.1st}$ of 35% and 50%, the higher combustion
274 efficiency and lower cooling loss are advantageous to the indicated thermal efficiency η_i.
275 With the $Q_{inj.1st}$ of 60%, the lower exhaust loss is advantageous to the indicated thermal
276 efficiency η_i. The combustion efficiency with the $Q_{inj.1st}$ of 60% is improved with the
277 advanced second injection, but the knocking limits the improvements.

278 Figure 8 plots the maximum pressure rise rate $(dp/d\theta)_{max}$ for different ratios of the
279 first injection quantity $Q_{inj.1st}$. The experiments were performed under the conditions in

Fig.7. At the second injection timings $\theta_{inj.2nd}$ before 2ºCA ATDC, the maximum pressure rise rate with the $Q_{inj.1st}$ at 60% was the highest, followed by that with the $Q_{inj.1st}$ at 35%, 50%, and 20%, decreasing in this order. With the $Q_{inj.1st}$ at 60%, the heat release due to the first and second HTOR overlap as the second injection timing advances, resulting in the increase of the ROHR seen in Fig.6. The maximum pressure rise rate with the $Q_{inj.1st}$ of 20% was lower than the others due to the late combustion, but here a further advance in the second injection was limited by the appearance of knocking. As the amount of the heat release in the first HTOR was small (see Fig.6), the ignition delay of the second injection was long, and a somewhat large amount of fuel remained until the second HTOR. This causes a large heat release with the advance of the combustion phase associated with the advanced second injection. Overall, this suggests that an appropriate amount of heat release due to the first HTOR is necessary to control the maximum pressure rise rate as with the $Q_{inj.1st}$ of 35% and 50%.

3.4 Comparison of the Impact of Ozone Concentration and Ratio of Fuel Injection Quantity under the Optimized Conditions

Figure 9 shows the relation among the combustion efficiency η_{comb}, ozone concentration X_{O3}, and the ratio of the first injection quantity $Q_{inj.1st}$. For all the data shown

297 here, the second injection timings achieving the maximum indicated thermal efficiency
298 were selected. It can be seen clearly that the combustion efficiency increases with the
299 increase of the ozone concentration for each level of the ratio of the first injection quantity.

300 Figure 10 shows the relation among the indicated thermal efficiency η_i, ozone
301 concentration X_{O3}, and the ratio of the first injection quantity $Q_{inj.1st}$. As in Fig.9, the
302 second injection timings achieving the maximum indicated thermal efficiency were
303 selected. The ozone concentration achieving the maximum indicated thermal efficiency
304 decreased with the increase in the $Q_{inj.1st}$. The indicated thermal efficiency increases with
305 the increase of the ozone concentration due to the increased combustion efficiency, but it
306 decreases when the ozone concentration exceeds a certain level. This trend can be
307 observed for each level of the ratio of the first injection quantity. This is due to a
308 combustion phasing advancement and increased cooling loss. There were very limited
309 differences in the maximum indicated thermal efficiency from the $Q_{inj.1st}$ of 35% to 60%.
310 Recall that, however, in the case of $Q_{inj.1st}$ of 60%, the operation achieving high indicated
311 thermal efficiency was accompanied by the high $(dp/d\theta)_{max}$.

312 Figure 11 shows the relation among the exhaust emissions, ozone concentrations X_{O3},
313 and the ratio of the first injection quantity $Q_{inj.1st}$. The smoke and NO_x emissions increased
314 with increases in the X_{O3} and the $Q_{inj.1st}$. Increases in the X_{O3} and $Q_{inj.1st}$ increased the heat

315 release in the first HTOR, and advanced the timing of the first HTOR, increasing the in-
316 cylinder gas temperature and the NO_x formation rate. Figure 12 shows the smoke
317 concentration vs. the ignition delay of the second injection $\tau_{ign.2nd}$, where all the data
318 acquired in the present experiments are plotted. The data acquired under the same
319 conditions as in Fig.11 are shown as filled (solid) symbols. Where the ignition delay was
320 difficult to determine, when there was simultaneous ignition of the first and second
321 injections, the experiment data is not plotted in the figure. The smoke emissions occurred
322 with the $\tau_{ign.2nd}$ shorter than 6ºCA; as the larger quantity of the first injection resulted in
323 the shorter $\tau_{ign.2nd}$, the smoke emissions increased with the increase of the X_{O3} and $Q_{inj.1st}$.

324 **3.5 Comparison with Conventional Diesel Combustion**

325 The engine performance and the exhaust emissions of GCI with the ozone addition
326 are next compared with those of conventional diesel combustion (CDC). The
327 experimental conditions of the conventional diesel combustion are detailed in Table 3.
328 The total injection quantity is slightly increased compared to the PRF90, to correct the
329 differences in the lower heating values. The other conditions were identical to those in
330 Table 2. As a preliminary experiment, the injection timings and the pilot injection amount
331 which achieved the maximum indicated thermal efficiency were determined while

maintaining the crank angle interval between the pilot and main injections at 8ºCA at the injection pressure p_{inj} of 80 MPa, at this condition the injection pressure was then changed from 80 MPa to 200 MPa, without other changes in the experimental conditions.

Figure 13 plots the profiles of the ROHR between GCI with the ozone addition and CDC with the different injection pressures. The operation with the $Q_{inj.1st}$ of 35%, the X_{O3} of 60 ppm, and the $\theta_{inj.2nd}$ of TDC was selected as the best GCI condition in this study. Compared at the p_{inj} of 80 MPa, GCI with the ozone addition presented a ROHR that was higher than CDC, representing the premixed combustion nature. The increase of the p_{inj} in CDC increased the ROHR of the pilot and main injections, reducing the combustion periods.

Figure 14 shows the indicated thermal efficiency η_i of CDC, compared with the best GCI operations derived from Fig.10. Compared at the same injection pressure of 80 MPa, the differences of the indicated thermal efficiency between CDC and GCI with the $Q_{inj.1st}$ of 35% and 60% are smaller than 1%, but increased with the increase of the injection pressure of CDC.

Figure 15 shows the trade-off relationship between the smoke and NO_x emissions. Here, the data shown in Fig.11 are plotted for comparison purposes. CDC with the injection pressure of 80 MPa generated the very high smoke concentration as well as the

slightly higher NO_x. Increasing the injection pressure up to 200 MPa in CDC, the smoke decreased dramatically, accompanied by the increase of NO_x. This result demonstrates that GCI assisted by ozone offers operation with the very low smoke and NO_x emissions.

4. Conclusions

The present study added ozone (O_3) to a gasoline compression ignition (GCI) engine, aiming to control the ignition timing and combustion progress. A two-stage fuel injection with very early injection and late injection close to top dead center was adapted to utilize O-radicals decomposed from the O_3 before the recombination reaction reduces them to O_2. The first injection quantity, the second injection timing as well as the O_3 concentration were varied to explore the optimum operation conditions at medium loads with a single cylinder GCI engine. Further, the engine performance and exhaust emissions with GCI were compared with conventional diesel combustion operation. The conclusions may be summarized as follows:

1. The GCI operation with a smaller amount of first injection results in combustion with lower combustion efficiency, so that higher ozone concentrations are required to increase combustion efficiency and to attain higher indicated thermal efficiency.
2. For each level of the ratio of the first injection quantity, with the increase of the ozone

concentration, the combustion efficiency increases, and the combustion phasing advances, accompanied by the increase of the cooling loss. Due to the balance between the combustion efficiency and the cooling loss, he indicated thermal efficiency has a local maximum value with respect to the ozone concentration.

3. The GCI operation without ozone is accompanied by a higher maximum pressure rise rate due to the simultaneous ignition of the first and second injection fuels. With an appropriate amount of first injection and ozone addition, the high temperature oxidation reactions of the first and second injection fuels occur in two stages, decreasing the maximum pressure rise rate.
4. The increase of the ozone concentration and the first injection quantity increase the rate of heat release caused by the high temperature oxidation of the first injection fuel. This increases the in-cylinder temperature and NO_x emissions, and decreases the ignition delay of the second injection, accompanied by the increase of the smoke emissions.
5. The indicated thermal efficiency of GCI assisted with ozone is slightly lower than that of the conventional diesel combustion, but GCI assisted with ozone is advantageous to the smoke and NO_x emissions.

385 The present study produced O_3 from pure oxygen on a trial basis. According to the
386 previous study by Inoue et al. who developed an intake in-line ozonizer, the ozone
387 enrichment in the order of 60 ppm is technically viable with air [26]. Estimated by
388 reference to this study [26], the energy loss due to the ozone production is about 1% in
389 the engine operation condition employed in this study. Further improvements in the
390 efficiency are still required.

391 **Acknowledgements**

392 This work was supported by JSPS Grants-in-Aid for Scientific Research (c) Number
393 19K04208.

394

395 **5. References**

396 [1] Dec, J. E., “A Conceptual Model of DI Diesel Combustion Based on Laser-Sheet
397 Imaging,” SAE Technical Paper, No.970873, 1997.
398 [2] Kosaka, H., Aizawa, T. and Kamimoto, T., “Two-dimensional Imaging of Ignition and
399 Soot Formation Processes in a Diesel Flame,” International Journal of Engine
400 Research, Vol.6, Issue 1, pp.21-42, 2005.
401 [3] Siebers, D. and Higgins, B., "Flame Lift-Off on Direct-Injection Diesel Sprays under
402 Quiescent Conditions," SAE Technical Paper 2001-01-0530, 2001.
403 [4] Higgins, B. and Siebers, D., "Measurement of the Flame Lift-Off Location on DI
404 Diesel Spray using OH Chemiluminescence," SAE Technical Paper 2001-01-0918,
405 2001.

406 [5] Siebers, D., Higgins, B. and Pickett, L., “Flame Lift-Off on Direct-Injection Diesel
407 Fuel Jets: Oxygen Concentration Effects,” SAE Technical Paper 2002-01-0890, 2002.
408 [6] Pickett, L., Siebers, D. and Idicheria, C., “Relationship between Ignition Processes
409 and the Lift-Off Length of Diesel Fuel Jets,” SAE Technical Paper 2005-01-3843,
410 2005.
411 [7] Yasutomi, K., Mueller, C. J., Pickett, L. M. and Skeen, S. A., “Investigation of the
412 Spray and Combustion Characteristics of Four Multi-Component Diesel Surrogates
413 Fuels Relative to Their Commercial Target Fuel,” THIESEL 2018 Conference on
414 Thermo- and Fluid Dynamic Processes in Direct Injection Engines, 2018.
415 [8] Kalghatgi, G., Risberg, P., and Ångström, H., “Advantages of Fuels with High
416 Resistance to Auto-ignition in Late-injection, Low-temperature, Compression
417 Ignition Combustion," SAE Technical Paper 2006-01-3385, 2006.
418 [9] Kalghatgi, G., Risberg, P., and Ångström, H., "Partially Pre-Mixed Auto-Ignition of
419 Gasoline to Attain Low Smoke and Low NOx at High Load in a Compression Ignition
420 Engine and Comparison with a Diesel Fuel," SAE Technical Paper 2007-01-0006,
421 2007.
422 [10] Hanson, R., Splitter, D., and Reitz, R., “Operating a Heavy-Duty Direct Injection
423 Compression-Ignition Engine with Gasoline for Low Emissions,” SAE Technical
424 Paper 2009-01-1442, 2009.
425 [11] Manente, V., Johansson, B., and Cannella, W., “Gasoline Partially Premixed
426 Combustion, the Future of Internal Combustion Engines?,” International Journal of
427 Engine Research, Vol.12, Issue 3, pp.194-208, 2011.
428 [12] Ra, Y., Loeper, P., Andrie, M., Krieger, R., Foster, D., Reitz, R., and Durrett, R.,
429 “Gasoline DICI Engine Operation in the LTC Regime Using Triple-pulse Injection,”
430 SAE Int. J. Engines 5(3), 2012.
431 [13] Sellnau, M. C., Sinnamon, J., Hoyer, K., and Husted, H., “Full-time Gasoline Direct-
432 injection Compression Ignition (GDCI) for High Efficiency and Low NOx and PM,”
433 SAE Int. J. Engines 5(2), 2012.
434 [14] Nishida, H. and Tachibana, T., “Homogeneous Charge Compression Ignition of
435 Natural Gas/Air Mixture with Ozone Addition,” Journal of Propulsion and Power,
436 Vol.22, No.1, pp.151-157, 2006.
437 [15] Mohammadi, A., Kawanabe, H., Ishiyama, T., Shoji M. and Komada, A., “Study on
438 Combustion Control in Natural-Gas PCCI Engines with Ozone Addition into Intake
439 Gas,” SAE Technical Paper 2006-01-0419, 2006.
440 [16] Schönborn, A., Hellier, P., Aliev, A E. and Ladommatos, N., “Ignition Control of
441 Homogeneous-Charge Compression Ignition (HCCI) Combustion Through

442 Adaptation of the Fuel Molecular Structure by Reactions with Ozone," Fuel, Vol.89,
443 Issue 11, pp.3178-3184, 2010.
444 [17] Foucher, F., Higelin, P., Mounaïm-Rousselle, C. and Dagaut, P., "Influence of Ozone
445 on the Combustion of n-heptane in a HCCI Engine," Proc. the Combustion Institute,
446 Vol.34, Issue 2, pp.3005-3012, 2013.
447 [18] Masurier, J.-B., Foucher, F., Dayma, G. and Dagaut, P., "Investigation of iso-Octane
448 Combustion in a Homogeneous Charge Compression Ignition Engine Seeded by
449 Ozone, Nitric Oxide and Nitrogen Dioxide," Proc. the Combustion Institute, Vol.35,
450 Issue 3, pp.3125-3132, 2015.
451 [19] Heimerl, J. M. and Coffee, T. P., "The Detailed Modeling of Premixed, Laminar
452 Steady-State Flames. I. Ozone," Combustion and Flame, Vol.39, Issue 3, pp.301-315,
453 1980.
454 [20] Yamada, H., Yoshii, M. and Tezaki, A., "Chemical Mechanistic Analysis of Additive
455 Effects in Homogeneous Charge Compression Ignition of Dimethyl Ether," Proc. the
456 Combustion Institute, Vol.30, Issue 2, pp.2773-2780, 2005.
457 [21] Ekoto, I. and Foucher, F., "Mechanisms of Enhanced Reactivity with Ozone Addition
458 for Advanced Compression Ignition," SAE Technical Paper 2018-01-1249, 2018.
459 [22] Kobashi, Y., Wang, Y., Shibata, G., Ogawa, H. and Naganuma, K., "Ignition Control
460 in a Gasoline Compression Ignition Engine with Ozone Addition Combined with a
461 Two-stage Direct-injection Strategy," Fuel, Vol.249, pp.154-160, 2019.
462 [23] Kokjohn, S. L., Hanson, R. M., Splitter, D. A. and Reitz, R. D., "Fuel Reactivity
463 Controlled Compression Ignition (RCCI): A Pathway to Controlled High-Efficiency
464 Clean Combustion," International Journal of Engine Research, Vol.12, Issue 3,
465 pp.209-226, 2011.
466 [24] Kobashi, Y., Tanaka, D., Maruko, T., Kato, S., Kishiura, M., and Senda, J., "Effects
467 of Mixedness and Ignition Timings on PCCI Combustion with a Dual Fuel
468 Operation," SAE Technical Paper 2011-01-1768, 2011.
469 [25] Pinazzi, P. M. and Foucher, F., "Potential of Ozone to Enable Low Load Operations
470 of a Gasoline Compression Ignition (GCI) Engine," SAE Technical Paper 2017-01-
471 0746, 2017.
472 [26] Inoue, T., Tamida, T., Hashimoto, T., Wada, N., Nakagawa, A., Sakashita, T., Wada,
473 K. and Honda, T., "The development of intake in-line type ozonizer for application
474 to HCCI combustion", Transactions of Society of Automotive Engineers of Japan,
475 Vol.48, No.4 (2017), pp.827-832 (in Japanese).

Table 1 Specifications of the test engine

Bore x Stroke [mm]		98 x 110
Displacement [cm^3]		830
Compression ratio [-]		17.6
Injection nozzle	Spray included angle [º]	155
	Number of nozzle hole	8
	Nozzle hole diameter [mm]	0.125

Table 2 Experimental conditions for gasoline compression ignition (GCI) with ozone addition

Fuel	PRF90
Engine rotation speed [rpm]	1200
Intake oxygen concentration [%]	15
Intake air temperature [ºC]	60
Intake air pressure [kPa (abs.)]	120
Intake O_3 concentration X_{O3} [ppm]	0 to 360
Fuel injection pressure p_{inj} [MPa]	80
First injection timing $\theta_{inj.1st}$ [ºCA ATDC]	-68
Second injection timing $\theta_{inj.2nd}$ [ºCA ATDC]	-6 to 6
Ratio of first injection quantity $Q_{inj.1st}$ [%]	20 to 60
Total injection quantity [mg]	29
IMEP [MPa]	≈ 0.67

Table 3 Experimental conditions for conventional diesel combustion (CDC)

Fuel	JIS No.2 Diesel fuel
Fuel injection pressure p_{inj} [MPa]	80, 120, 160, 200
Pilot injection timing $\theta_{inj.1st}$ [ºCA ATDC]	-10
Main injection timing $\theta_{inj.2nd}$ [ºCA ATDC]	-2
Pilot injection quantity [mg]	1
Main injection quantity [mg]	29

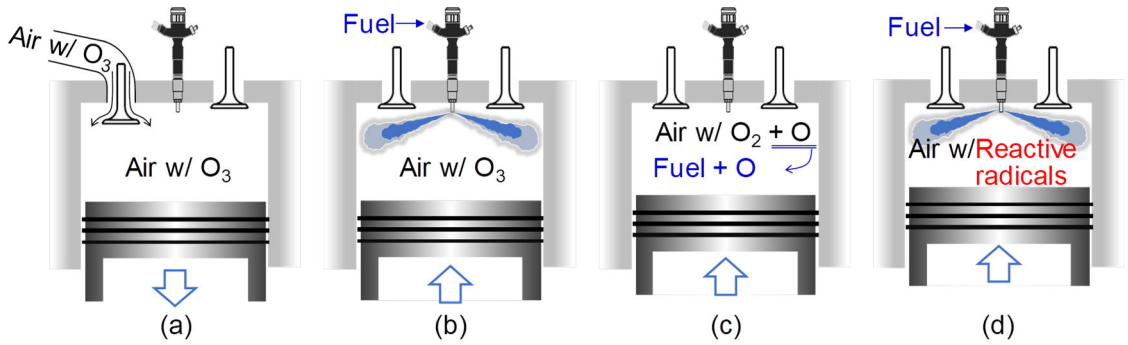

Figure 1 Schematic of the combustion control methodology with ozone addition and two-stage injection, proposed in this study

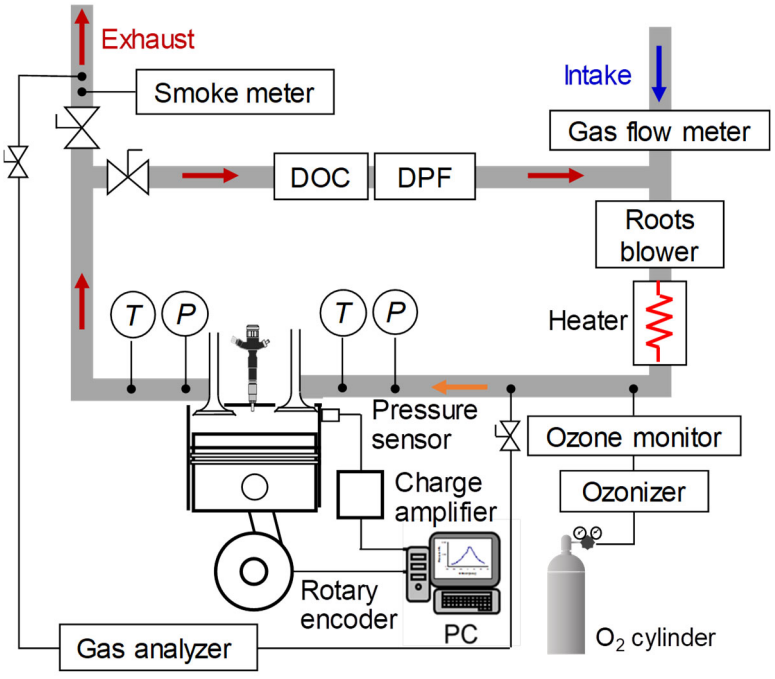

Figure 2 Illustration of the experimental setup

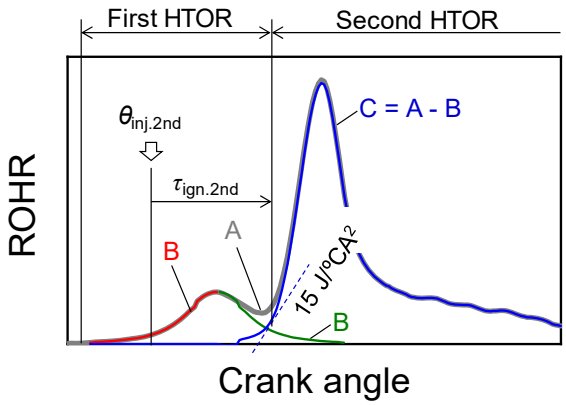

Figure 3 Definition of the ignition delay of the second injection

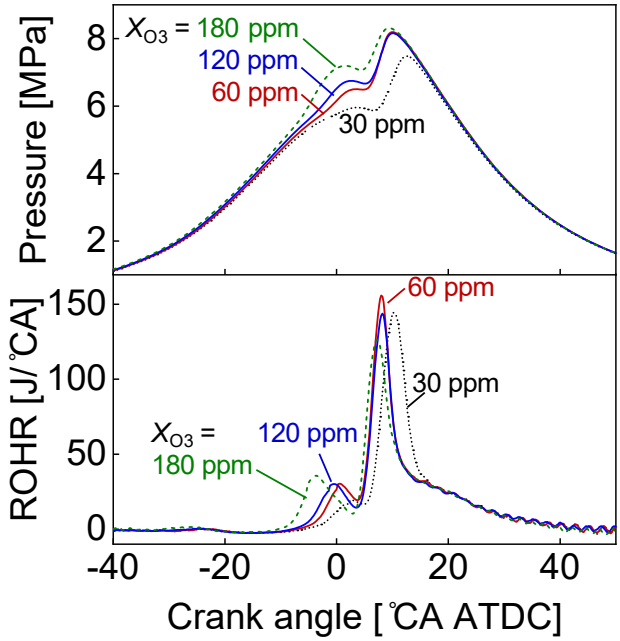

Figure 4 Profiles of the in-cylinder pressure and rate of heat release (ROHR), changing with the ozone concentration X_{O3} ($Q_{inj.1st}$ = 35%, $\theta_{inj.2nd}$ = TDC)

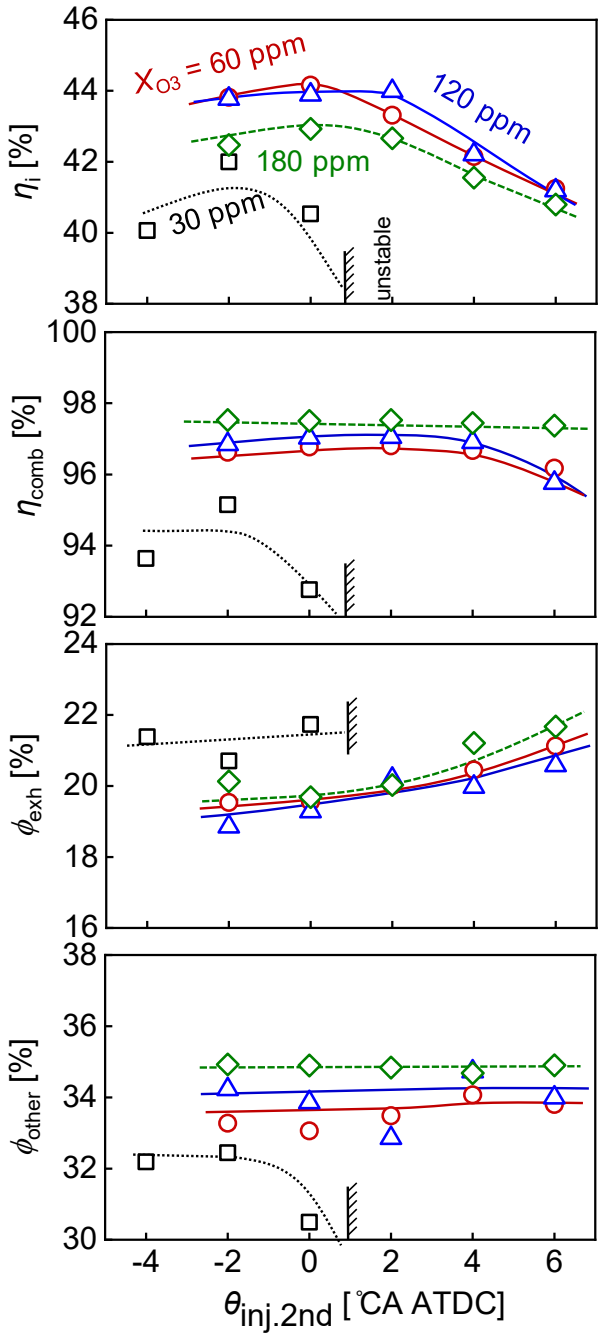

Figure 5 Effects of the ozone concentration X_{O3} on the indicated thermal efficiency η_i, combustion efficiency η_{comb}, exhaust loss ϕ_{exh}, and other loss ϕ_{other} ($Q_{inj.1st}$ = 35%)

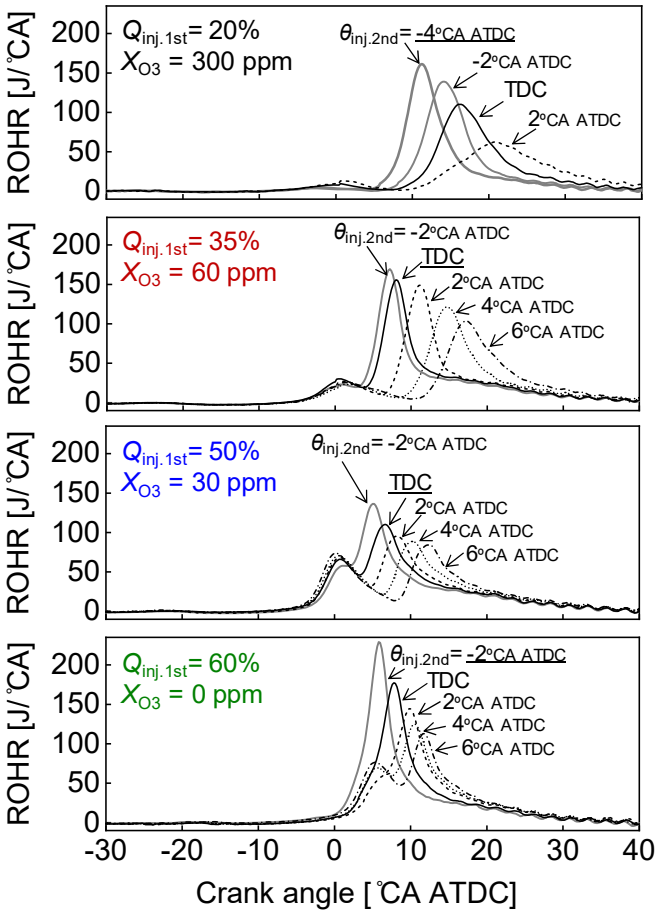

Figure 6 Profiles of the rate of heat release (ROHR), changing with the second injection timing $\theta_{inj.2nd}$
Ozone concentrations achieving high indicated thermal efficiency were selected

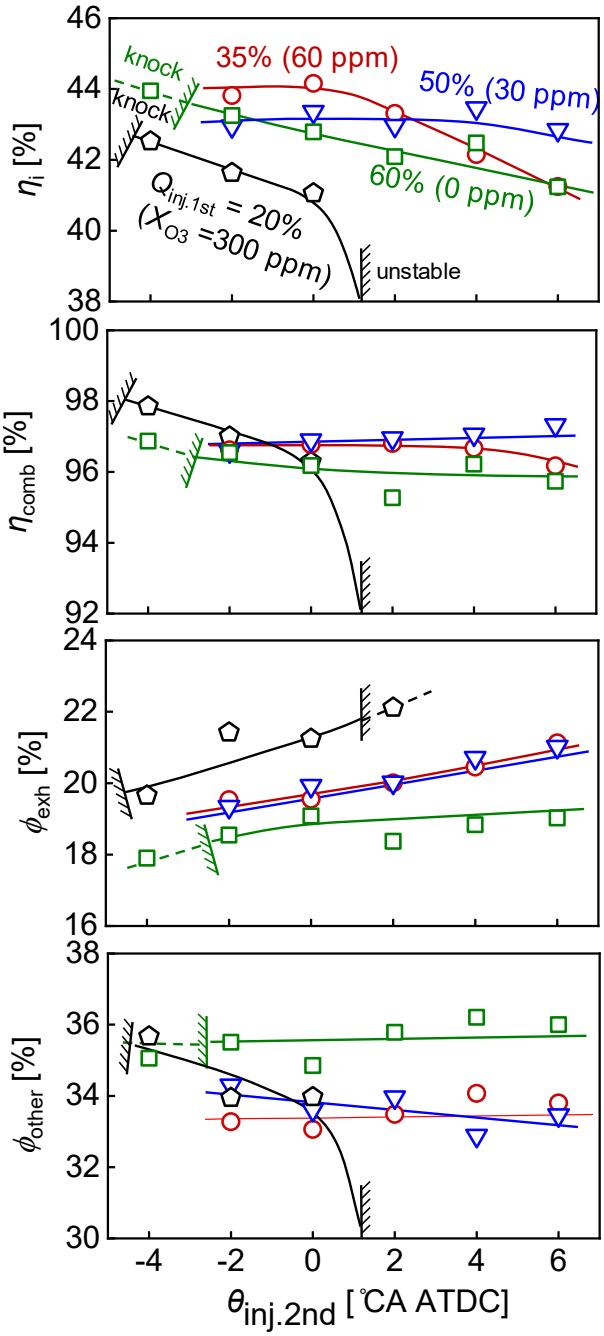

Figure 7 Comparison of the indicated thermal efficiency η_i, combustion efficiency η_{comb}, exhaust loss ϕ_{exh}, and other losses ϕ_{other} between the ratio of the first injection quantity $Q_{inj.1st}$

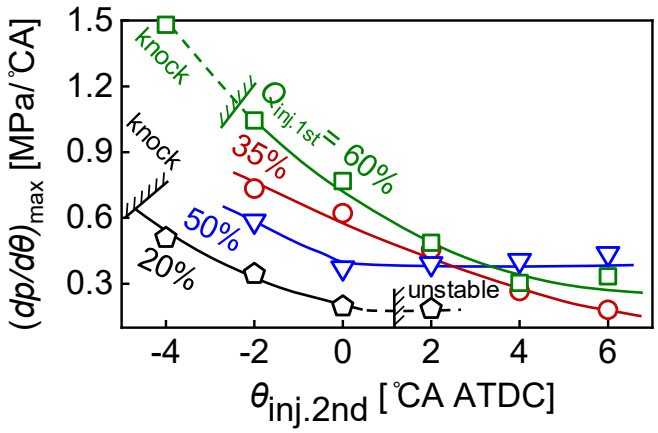

Figure 8 Comparison of the maximum pressure rise rate between the ratio of the first injection quantity $Q_{\mathrm{inj.1st}}$

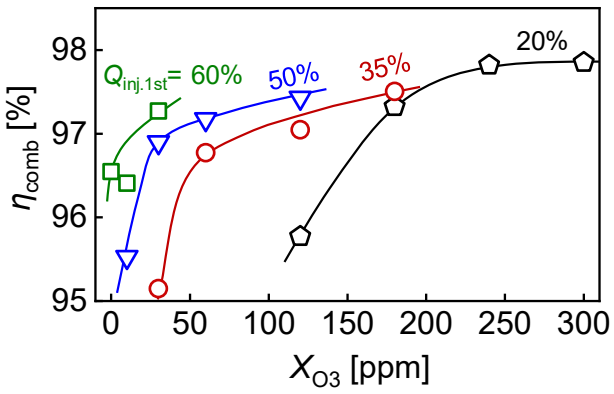

Figure 9 Effects of the ozone concentration X_{O3} and the ratio of the first injection quantity $Q_{inj.1st}$ on the combustion efficiency η_{comb}
The second injection timings achieving the maximum indicated thermal efficiency were selected

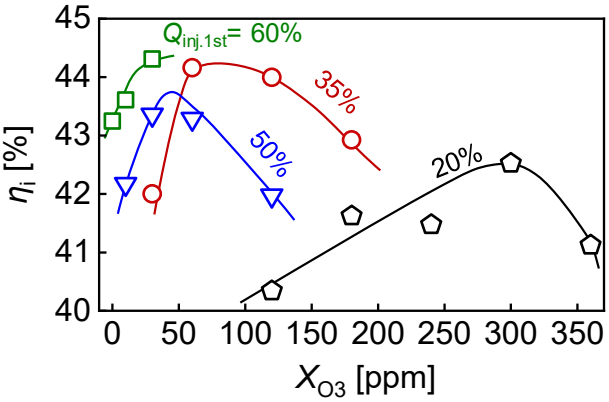

Figure 10 Effects of the ozone concentration X_{O3} and the ratio of the first injection quantity $Q_{inj.1st}$ on the indicated thermal efficiency η_i
The second injection timings achieving the maximum indicated thermal efficiency were selected

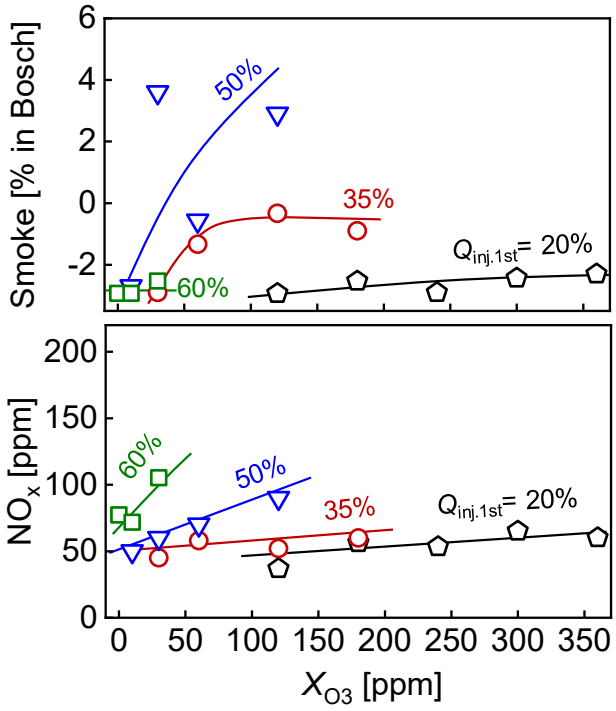

Figure 11 Effects of the ozone concentration X_{O3} and the ratio of the first injection quantity $Q_{inj.1st}$ on the smoke and NO_x emissions
The second injection timings achieving the maximum indicated thermal efficiency were selected

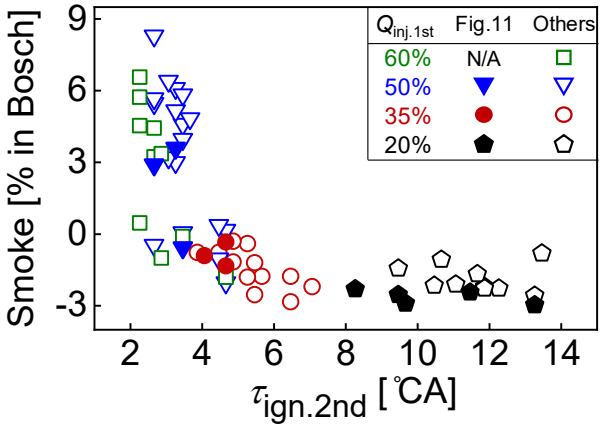

Figure 12 Smoke concentration vs. the ignition delay of the second injection $\tau_{ign.2nd}$
All the data points, except for the conditions where the ignition delay was difficult to determine (due to overlapping), were plotted

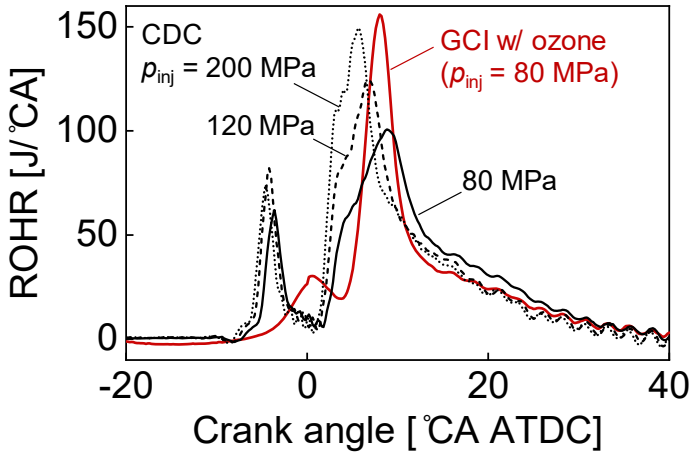

Figure 13 Comparison of profiles of the rate of heat release (ROHR) between the gasoline compression ignition (GCI) with ozone addition and conventional diesel combustion (CDC) with different injection pressures p_{inj}

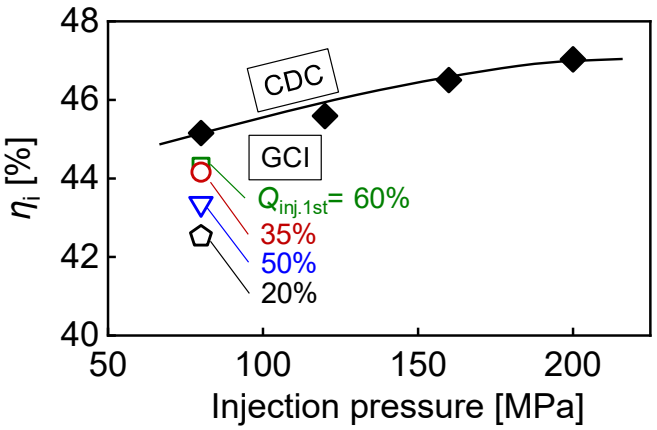

Figure 14 Comparison of the indicated thermal efficiency η_i between the gasoline compression ignition (GCI) with ozone addition and conventional diesel combustion (CDC) with different injection pressures p_{inj}
The GCI data were derived from Fig.10, selecting the maximum indicated thermal efficiency with respect to each of the quantities of the first injection

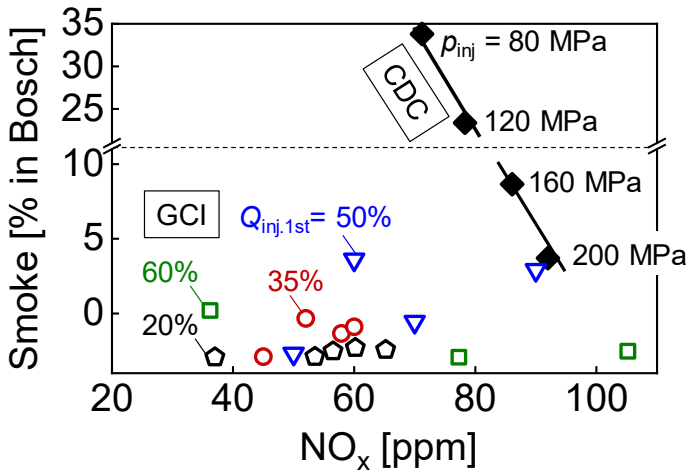

Figure 15 Comparison of the smoke and NO_x emissions between the gasoline compression ignition (GCI) with ozone addition and conventional diesel combustion (CDC) with different injection pressures p_{inj}
The GCI data were derived from Fig.11